The Abdus Salam
International Centre for Theoretical Physics

United Nations
Educational, Scientific and
Cultural Organization

IAEA
International Atomic Energy Agency

1867-53

College of Soil Physics

22 October - 9 November, 2007

THE INFLUENCE OF TILLAGE AND AND OF COMPRESSION UPON SOIL PHYSICAL PROPERTIES

Miroslav Kutilek
Nad Patankou 34
160 00 Prague 6
Czech Republic

ICTP TRIESTE
COLLEGE ON SOIL PHYSICS 2007

THE INFLUENCE OF TILLAGE AND AND OF COMPRESSION UPON SOIL PHYSICAL PROPERTIES

LECTURE NOTES

Mirek Kutílek,

1. INTRODUCTION

The main factors influencing the change of the soil physical properties:

1. Destruction of soil structure is related in a broad sense to soil degradation. Desaggregation in A horizon is caused mainly by the combination of mechanical action of agricultural machinery and by the decrease of C org. especial by the decrease of components of stabile soil humus (e.g. humic acids) after tens of years of intensive agricultural use of soils. The desaggregation in deeper horizons is related partly to the degradation of the whole soil profile, partly it is the result of the use of heavy machinery.
2. Soil compaction is the result of the weight and dynamic action of agricultural machinery and tillage operations. The compaction may be limited just to the surface horizon, but after a long term use of heavy machinery it may reach up to the depth of 60 or 70 cm. This deep layers compaction is not simply ameliorated, in some instances the compaction is nearly irrreversible.
3. The substantial change of the chemical composition of the soil solution may cause a change of the ζ potential. The fine soil particles are peptized, the soil aggregation is not possible and the soil hydraulic conductivity is then substantially reduced, as it was shown in Lecture Notes on Saturated and Unsaturated Flow. The change of the soil solution is either due to deposition of wastes or due to the inappropriate irrigational practices in arid zones.

The items 1. and 2. will be discussed in detail. We use the following tools for characterizing soil physical properties by the study of the soil porous system (SPS)

(i) Empirical soil water retention curve SWRC *S(h)*, or $\theta(h)$ and its derivative curve with $r = a/h$ is the empirical pore size distribution.

(ii) The minimum minimorum on the derivative curve to empirical soil water retention curve h_A separates the matrix (indexed by 1) from the structural domain (indexed by 2).

(iii) Model of lognormal pore size distribution *g(r)*

$$g(r) = \frac{\theta_S - \theta_R}{\sigma r\sqrt{2\pi}} \exp\left\{ - \frac{[\ln(r / r_m)]^2}{2\sigma^2} \right\} \qquad (1)$$

(iv) SWRC of bi-modal soils with pore size distribution modeled by (1)

$$S_i = \frac{1}{2} erfc\left[\frac{\ln(h_i / h_{mi})}{\sigma_i \sqrt{2}} \right] \qquad (2)$$

$$S_i = \frac{\theta_i - \theta_{Ri}}{\theta_{Si} - \theta_{Ri}} \tag{3}$$

and $\theta = \theta_1 + \theta_2$ when $i = 1$ is for matrix pores and $i = 2$ for structural pores.

(v) Unsaturated hydraulic conductivity function of bi-modal soils with pore size distribution modeled by (1)

$$K_{Ri} = S_i^{\alpha i} \left\{ \frac{1}{2} erfc \left[(\ln \frac{h_i}{h_{mi}}) \frac{1}{\sigma_i \sqrt{2}} + \frac{\beta_i \sigma_i}{\sqrt{2}} \right] \right\}^{\gamma i} \tag{4}$$

$K_R = K/K_S$ and when $i = 1$ is for matrix pores and $i = 2$ for structural pores. And $K = K_1 + K_2$.

K_S is saturated hydraulic conductivity and h is the pressure head (potential), θ is the volumetric soil water content, r is the pore radius, r_m is the geometric mean radius, σ is the standard deviation, θ_R is the residual soil water content when the liquid flow is essentially zero, θ_S is the soil water content at saturation, i.e. at $h = 0$, S is the relative saturation, or parametric soil water content [dimensionless], h_m is the pressure head related to r_m, and *erfc* is the complementary error function. Parameters α, β, γ in (4) are assumable tortuosity and pore connectivity characteristics in Childs-Fatt-Burdin-Mualem equation

$$K_R = S^{\alpha} \left[\frac{\int_0^r r^{\beta} g(r) dr}{\int_0^{\infty} r^{\beta} g(r) dr} \right]^{\gamma} \tag{5}$$

2. THE ROLE OF SOIL STRUCTURE (Kutílek, 2004)

The role of soil structure was studied on Gleyic Hapludalf loamy soil developed on fluvial loess deposits. The measurements were performed on two locations at a depth of 15 cm in the Ap-horizon. One was with a moderately developed structure, denoted by S15 and the other one was on a compacted path by wheel track with distinctly destroyed structure, denoted by D15. At the first location, the measurements were also performed in the B-horizon at the depth 60 cm (S60).

The retention curve for each of the soil horizon was plotted and the derivative curve to the retention curve was used in order to separate the two domains of matrix (indexed by 1) and of structural pores (indexed by 2), Fig. 1. At the minimum of the derivative curve, the value h_A was estimated. It separates the two domains. Physically, it is the air entry value of the matrix domain. For each domain a separate retention curve was reconstructed. Fig. 2. Parameters of Eq. (2) and (3) were obtained by a fitting procedure to the measured data. They are together with h_A in the Table 1, where SPS1 denotes matrix pores, SPS2 the structural pores.

Table 1

Soil	SPS	h_m	σ	θ_S	θ_R	h_A
S15	1	2460	1.5	0.318	0	60
	2	9.8	1.1	0.147	0	0
S60	1	1000	1.52	0.35	0	30
	2	13.8	0.84	0.079	0	0
D15	Mono	1450	2.03	0.405	0.08	0

If the structure is destroyed, the bi-modal system approaches the monomodal system and in this studied case, $h_A = 0$. The value of h_m was between h_{m1} of top A horizon and B horizon, but the structural domain disappeared totally.

Parameters $\alpha, \beta,$ were evaluated by fitting procedure for simplified assumption on $\gamma = 1$, according to Eq. (4), see the Table 2.

Table 2

Soil	SPS	h_A	α	β	γ
S15	1	60	1.0	2.3	1
	2	0	0.45	0.7	1
S60	1	30	-0.3	1.4	1
	2	0	-1.0	1.8	1
D15	Mono	0	-0.3	1.2	1

Parameters α, β in the equation for unsaturated conductivity are different for matrix and structural domains of the soil porous system. The configuration of pores is therefore also different in the two domains. The soil with the destroyed structure lacks the structural domain and the parameters α, β differ from the soil well aggregated.

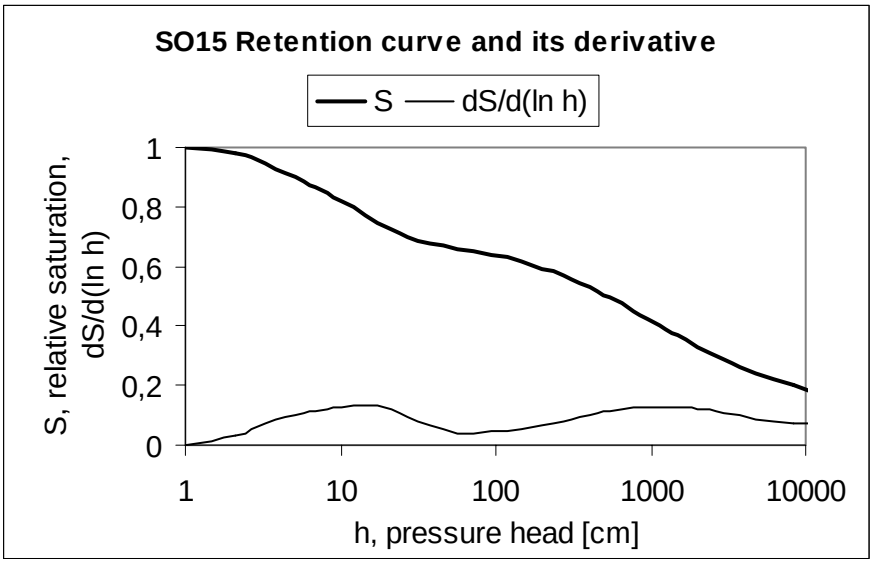

Fig. 1 Soil water retention curve of a well aggregated soil. Structural domain of pores is on the left side from the minimum on the derivative curve $h_A = 60$ cm, i.e. $1 > h > h_A$ and the matrix domain of pores is on right side of h_A, i.e. $h < h_A$.

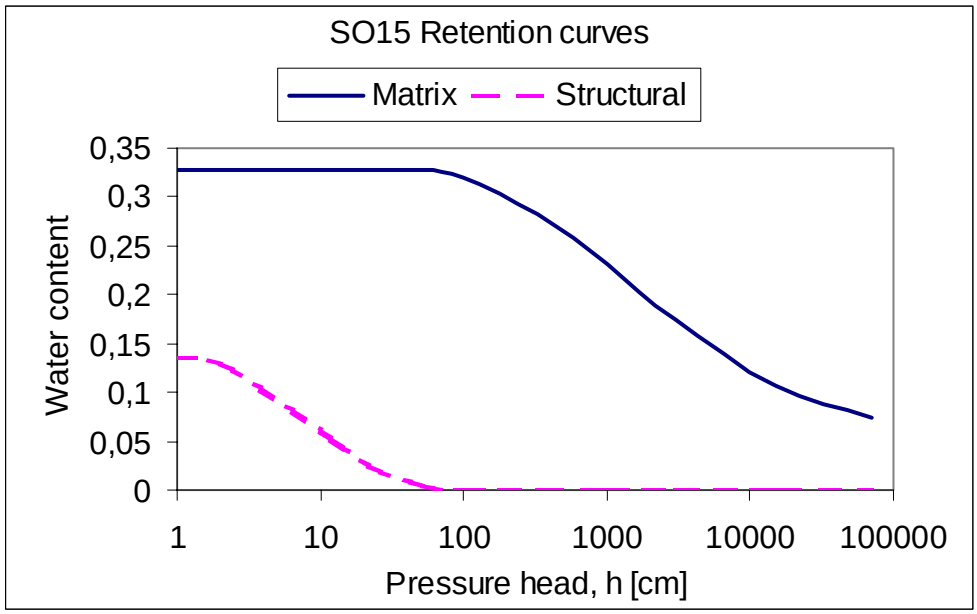

Fig. 2. Separation of two domains of SWRC: Matrix SWRC and structural SWRC in a well aggregated soil

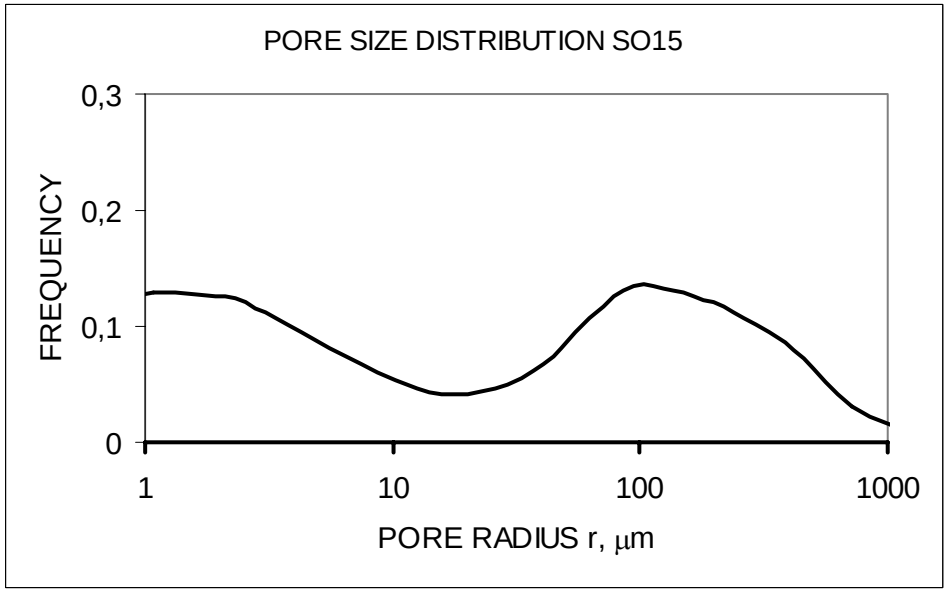

Fig. 3. Pore size distribution in a well aggregated soil. The peak on the right hand side belongs to structural domain, the peak on the left hand side belongs to the matrix domain.

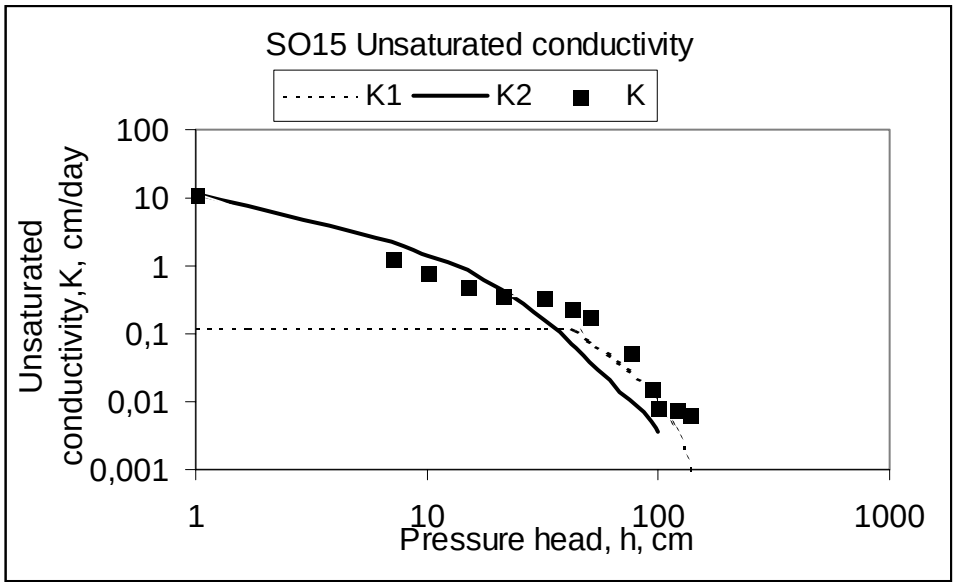

Fig. 4. The measured ■ unsaturated hydraulic conductivity of the well aggregated soil was transformed into conductivities of the structural domain and matrix domain by eq.(4). Preferential flow is realized in the structural domain and the structural conductivity function is indispensable for the solution of the preferential flow.

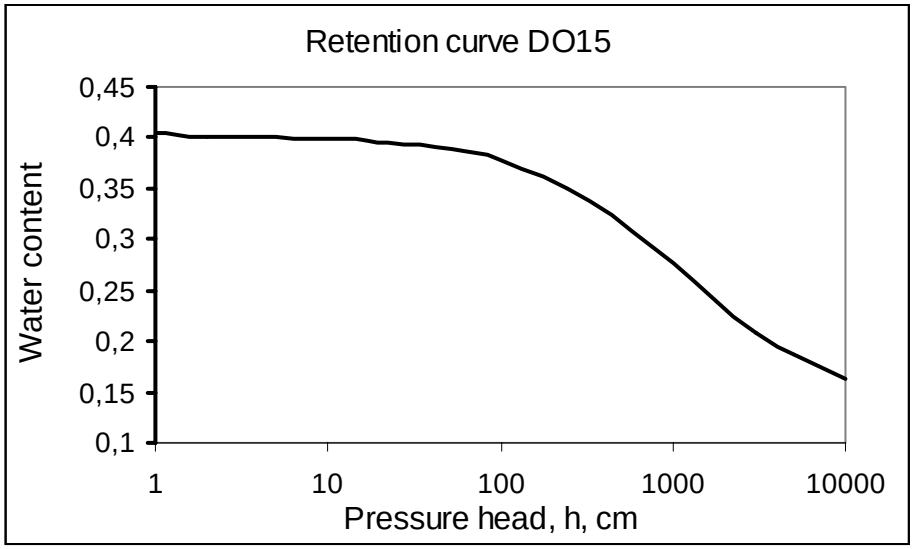

Fig. 5. Retention curve of the same soil as SO15, but the aggregates were mechanically destroyed. There is no indication of a separation of two domains. The structural domain is absent due to the loss of structure.

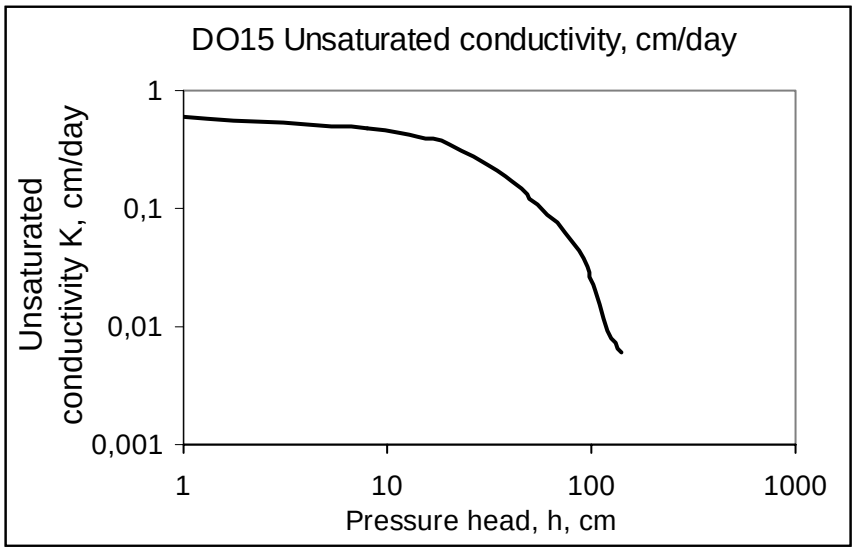

Fig. 6. Unsaturated conductivity of the same soil as SO15, but the aggregates were mechanically destroyed. Conductivity is by about one and half order of magnitude smaller than in aggregated soil in the wet domain, since the structural domain is absent.

3. THE CHANGE OF THE SOIL POROUS SYSTEM DUE TO COMPACTION (Kutilek, et al. 2006)

3.1. INTRODUCTION

Soil compaction influences soil water relations in a non-uniform way. Canarache (1984) has shown that compaction results in a decrease of water retention and Mapa et al. (1986) found that compaction reduces the macropores resulting in a decrease of water held at low suction. Assouline et al. (1997) analyzed the soil water retention curves of soils at compactions from 50 kPa to 1000 kPa using the Brooks and Corey equation. Their results confirm that changes in bulk density do not necessarily represent the effect of compaction on soil water retention properties and that there exists a reduction in the number of larger pores (up to pressure head h = -15000 cm) due to compaction. The change of water retention curve and of the pore size distribution was interpreted up to now by empirical limits of pore classes, as e.g. by effective porosity (pores characterized by h > -330 cm, Ahuja et al., 1984), macropores of diameter $D \geq 75$ μm (corresponding to $h \geq$ -40 cm, Brewer, 1964), eventually D > 750 μm with h > -4 cm (Clothier and White, 1981), or D > 1000 μm with h > -3 cm according to Luxmoore (1981), who has introduced mesoporosity with D = 10 to 1000 μm corresponding to h = -3 to -300 cm and microporosity with D < 10 μm, h < -300 cm. The concept of transmission pores with D = 50 – 500 μm (h in ranges of -6 to -60 cm) and storage pores with D = 0.5 – 50 μm (h = -60 to - 6000 cm, Greenland, 1981) was applied, too. Luxmoore has however stated that the operational boundary definitions between three soil porosity classes based on pressure and equivalent pore diameter may not necessarily be the best choice for all soils. Only recently the soil water retention curve was analyzed by the model of log-normal distribution in mono-modal soils by Leij et al. (2002) in their study on

dynamic modeling of the porous system. I am presenting a study on the change of pore size distribution when the lognormal model is applied to bi-modal soils.

3.2. MATERIALS AND METHODS

Undisturbed soil samples (100 cm^3) were taken from the A or Ap horizon in five locations of Greece with Mediterranean climate (Panayiotopoulos et al., 2003):

1. Loamy sand Entisol of poor structure development and low aggregate stability, under asparagus. Pre-compression stress is estimated as less than 100 kPa.
2. Sandy loam Entisol of poor structure development and low aggregate stability, under asparagus. The estimate of pre-compression stress is approximately 100 kPa.
3. Sandy clay loam Alfisol (Haploxeralf) with high aggregate stability, not cultivated for 15 years. The estimate of pre-compression stress is approximately 200 kPa.
4. Sandy loam Alfisol (Rhodoxeralf) with high aggregate stability, after winter wheat. Pre-compression stress is estimated as less than 100 kPa.
5. Clay loam Vertisol with high aggregate stability, not cultivated for 15 years. Pre-compression stress is estimated as less than 100 kPa.

Details on soil properties and on aggregate analysis were published by Panayiotopoulos et al. (2003 and 2004). The core samples were saturated by de-aerated 0.005 M $CaSO_4$, then equilibrated to -100 cm pressure head and stressed uni-axially at 100, 200 and finally at 300 kPa by static loading for 1 minute. The control sample (zero compression) and samples after compression were used for the determination of the soil water retention curves. The tension table with hanging water column was used for pressure heads -10, -20, -40 and -100 cm. For pressure heads -330, -1000, -10000 cm the pressure plate apparatus was applied. Finally, the water content of the air dried soil was related to -10^6 cm. The pressure head corresponds to air humidity 50% at the laboratory average temperature. The results were plotted in the graphical form of soil water retention curves by Panayiotopoulos et al. (2003).

In the present work, the experimentally determined data of the soil water retention curve $\theta(h)$ are first transformed into $S(h)$ according to Eq. (3). Then, a cubic spline function is fitted resulting in a smooth curve $S(\ln h)$ through the experimental data. It is assumed that θ_R is the water content of the air dried soil samples. Having a smooth curve $S(\ln h)$, the curve $\partial S(\ln(h))/\partial \ln(h)$ was calculated. The curve is identical to the pore size distribution if h is recalculated to equivalent pore radius r.

We have used following simplifications when recalculating the pressure head to the equivalent pore radius r: Soil pores were defined as cylindrical capillaries. The contact angle was taken as zero (complete wetting) and the surface tension of soil water was assumed to be equal to tabled value of water at 20^o C. Then $r = 1490/h$, with r in μm and h in cm (Kutílek and Nielsen, 1994).

There are typically two distinct peaks separated by the minimum with its lowest value at h_A on the derivative curve. For $0 > h > h_A$ the structural domain is considered and its characteristics are indexed by 2. For $h < h_A$ matrix domain is regarded, denoted by index 1. Graphical presentations of the procedures are demonstrated for loamy sand Entisol in Fig.1,

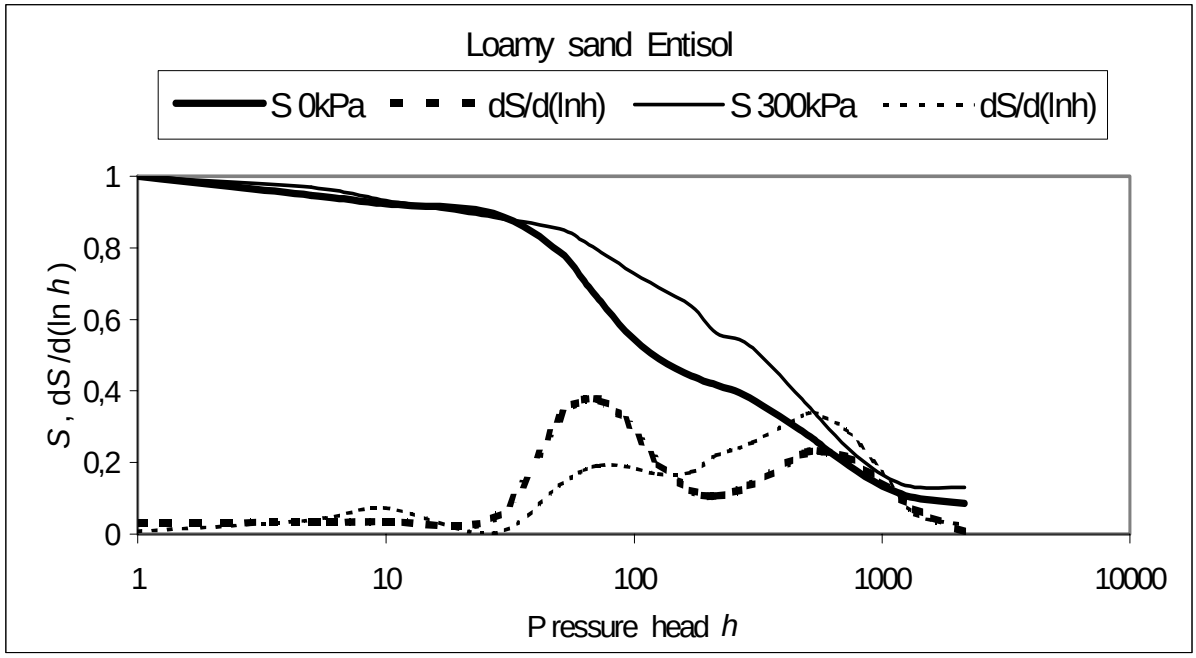

Fig. 1. Retention curves and their derivative curves for poorly aggregated Entisol without compression (0 kP) and after compression by 300 kPa.

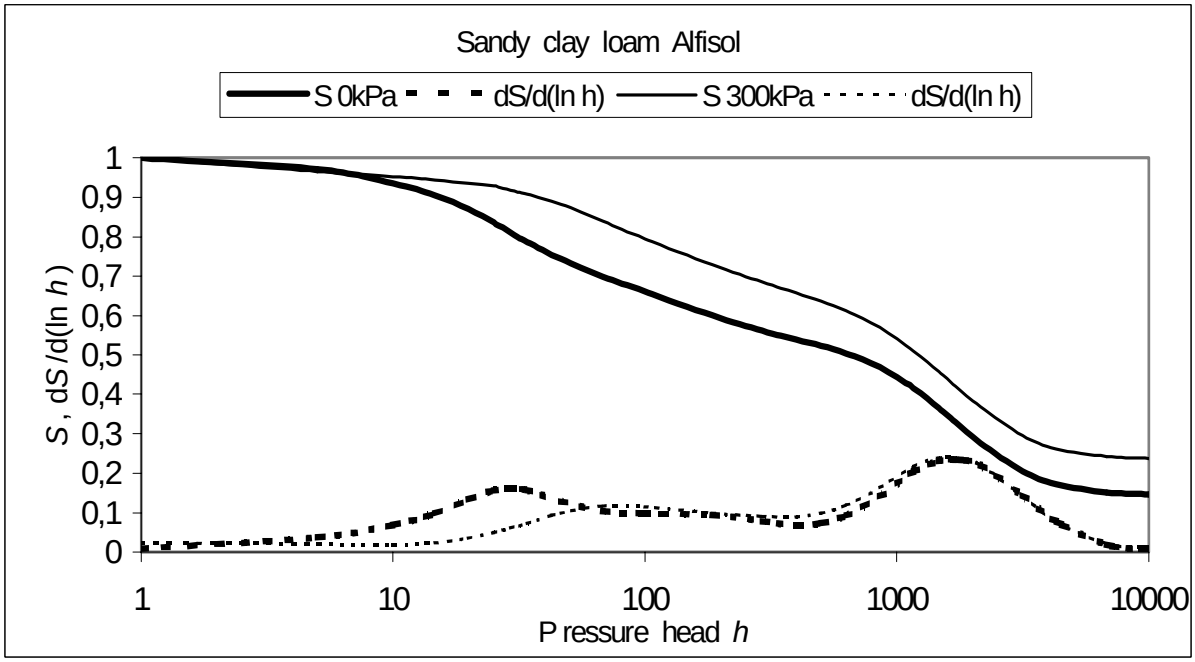

Fig. 2. Retention curves and their derivative curves for well aggregated Alfisol without compression (0 kP) and after compression by 300 kPa.

.

and for sandy clay loam Alfisol in Fig. 2. In both soils the curves of zero and 300 kPa compressive stress are plotted.

The crucial point in the present study was to find soil parameters in equations (2) and (3). This non-linear curves fitting was carried out by conjugate gradient method applied to finding minimum of a function f (*x*) of *n* variables, see Powell (1977, 1978). The spline

function covering the measured data range S (ln h) was divided into 180 equidistant sample points. The error of each of the sample points was calculated as a square of difference between the value S on the multiple spline function and the fitting function (2) at this point, when we are keeping condition described in detail in Lecture Notes "Hydraulic Functions of Soils Based Upon Characteristics of Porous System". The guessed starting values for the optimization h_{m1}, h_{m2}, σ_1, σ_2 were calculated as a mean and a standard deviation of the measured data S_i (ln h) for each of the domains. The Powell´s procedure provides a fast rate of convergence.

3.3 RESULTS AND DISCUSSION

3.3.1. Soil water retention curves

We computed smooth soil water retention curves $\theta(h)$ passing through all experimental points. Cubic spline procedure was used. After that, we transformed the standard forms of soil water retention curves $\theta(h)$ into parametric forms $S(h)$, where S is defined by Eq. (3) and h is plotted as logarithm. The example of loamy sand Entisol with poor structure without compression and after 300 kPa compression is in Fig.1. Derivative curves to retention curves are plotted in the same figure, too. A significant change of the retention curve due to compression is evident from both relationships, from $S(h)$ and from its derivative. There is a tendency to tri-modality after compression in the domain of structural pores. However, without micromorphological study we can not explain this phenomenon, which we observed in both Entisols after compression. The tri-modality is more distinct for the highest compression stress 300 kPa than for lower compression values. Another example of sandy clay loam Alfisol with a high aggregate stability is in Fig. 2. The retention curve is slightly changed due to the compression, but its shape is not significantly influenced by the compression, as it is evident from the derivative curves. Since the precompression stress of this Alfisol was estimated about 200 kPa, the retention curves of sandy loam Alfisol with precompression stress below 100 kPa are plotted in Fig. 3 together with derivative curves to

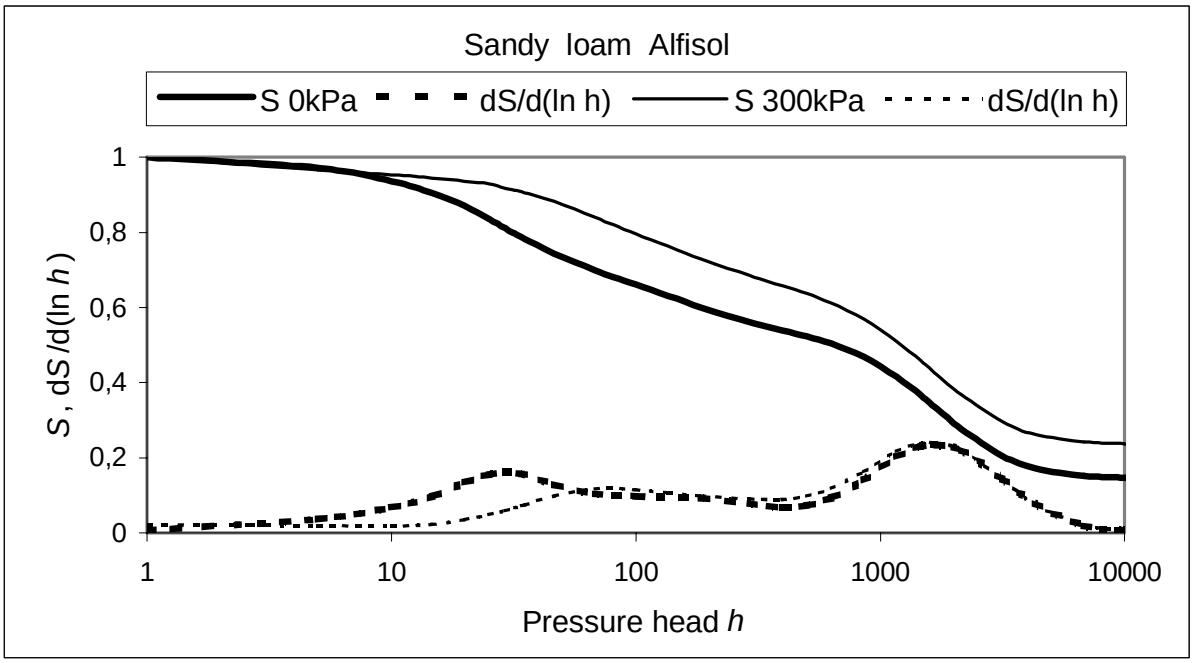

Fig. 3.

the retention curves. The change of the shape of the soil water retention curve due to compression is small likewise to sandy clay loam Alfisol. The precompression stress plays therefore a negligible role, if any, upon the change of the soil water retention curves in soils with well developed structure and high aggregate stability. On the other hand the low stability of aggregates in Entisols results in significant change of the shape of the soil water retention curve due to the compression.

3.3.2. Separation of structural and matrix domains

Based on the knowledge of relationships $\partial S(\ln(h))/\partial \ln(h)$ the value of h_A was determined, see the Table 1. It separates the structural and matrix domains. There is not an unambiguous change of this boundary between the two domains of pores due to compression. It is slightly decreasing in majority soils, in others it is increasing due to compression stress, but the change of h_A is relatively small. The values of h_A in all tested soils range between 136 and 585 cm of pressure head, or between 2.5 and 10.9 μm of equivalent pore radius. Tuller and Or (2002) assume that the matrix contains small pore sizes in the range of 10 to 0.1 μm. Our evaluation of experimental data confirms validity of their proposal. The broad range of h_A estimated in our research has an important consequence: The boundary between the soil pore categories can not be taken as a fixed value for all soils and all types of soil use. The classification of soil pores according to subjectively or "statistically" defined fixed boundary values as e.g. the definition of boundaries of transmission pores or meso-pores is therefore not appropriate.

Table 1. θ_S is saturated water content, θ_{S1}, θ_{S2} were obtained by optimization, index *1* is for the matrix, *2* for the structural saturated water contents, h_A is the pressure head separating the structural from the matrix domains.

Soil	Compressive stress, kPa	θ_S Measured	θ_{S1} Matrix	θ_{S2} Structural	h_A, cm
ENTISOL Loamy sand	0	0.621	0.266	0.355	215
	100	0.594	0.283	0.311	195
	200	0.572	0.316	0.256	190
	300	0.543	0.371	0.172	136
ENTISOL Sandy loam	0	0.60	0.314	0.286	585
	100	0.592	0.294	0.298	545
	200	0.588	0.329	0.259	562
	300	0.563	0.291	0.272	575
ALFISOL Sandy clay Loam	0	0.511	0.291	0.220	433
	100	0.506	0.303	0.203	373
	200	0.474	0.349	0.125	341
	300	0.468	0.327	0.141	368
ALFISOL Sandy loam	0	0.588	0.307	0.281	342
	100	0.570	0.317	0.253	398
	200	0.563	0.317	0.246	433
	300	0.551	0.340	0.211	369
VERTISOL Clay loam	0	0.656	0.416	0.240	365
	100	0.629	0.406	0.223	171
	200	0.580	0.383	0.197	373
	300	0.566	0.368	0.198	398

The compression has caused a decrease of the total porosity P_T, assuming $P_T = \theta_S$. The decrease of structural porosity $P_2 = \theta_{S2}$ is higher as compared to decrease of the total porosity θ_S, see Table 1. It indicates that the value of structural porosity is mainly influenced by compression. The matrix porosity $P_1 = \theta_{S1}$ is in majority of instances increasing with the increase of compression; in two soils it is slightly decreasing. This deviation is not definable from the measured soil characteristics.

Table 2

Relative values of total porosity P_{rT} , matrix porosity P_{r1} and structural porosity P_{r2}.

Soil	Compressive stress, kPa	P_{rT}	P_{r1}	P_{r2}
ENTISOL Loamy sand	0	1	1	1
	100	0.96	1.06	0.87
	200	0.92	1.19	0.72
	300	0.87	1.39	0.48
ENTISOL Sandy loam	0	1	1	1
	100	0.99	0.94	1.04
	200	0.98	1.05	0.91
	300	0.94	0.93	0.95
ALFISOL Sandy clay loam	0	1	1	1
	100	0.99	1.04	0.92
	200	0.93	1.20	0.57
	300	0.92	1.12	0.64
ALFISOL Sandy loam	0	1	1	1
	100	0.97	1.03	0.90
	200	0.96	1.03	0.88
	300	0.94	1.11	0.75
VERTISOL Clay loam	0	1	1	1
	100	0.96	0.98	0.93
	200	0.88	0.92	0.82
	300	0.86	0.88	0.83

In order to offer a simple information about the discussed change of the total porosity P_T, matrix porosity P_1 and structural porosity P_2 , we present Table 2 with relative values of porosity changes subject to compression. We denote $P_{rT} = P_{TC} / P_{T0}$ where P_{T0} is the total porosity of the control at zero compression and P_{TC} is the total porosity at the given compression stress. P_{r1} and P_{r2} are computed similarly.

3.3.3. Pore size distribution: Experimental data

The change of the pore size distribution due to the 300 kPa compression in two soils with low and high aggregate stability is documented in Figs. 4 and 5. The curves were derived from the derivative curves in Figs 1 and 2, when the pressure head h was replaced by the equivalent pore radius r, μm. The change of the pore size distribution in Entisol with low aggregate stability is large in both domains, Fig. 4. There is a tendency to tri-modal distribution in Entisols due to the compression. In Alfisol with well developed and stabile

structure, the change of the pore size distribution is mainly in structural domain, while it is negligible in the matrix domain, Fig. 5.

Fig. 4.

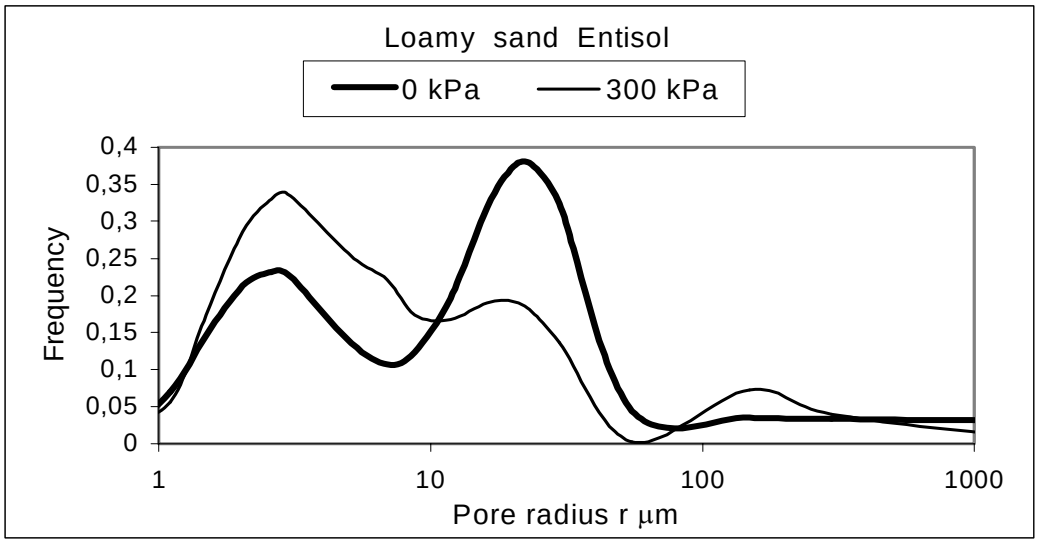

Fig. 5.

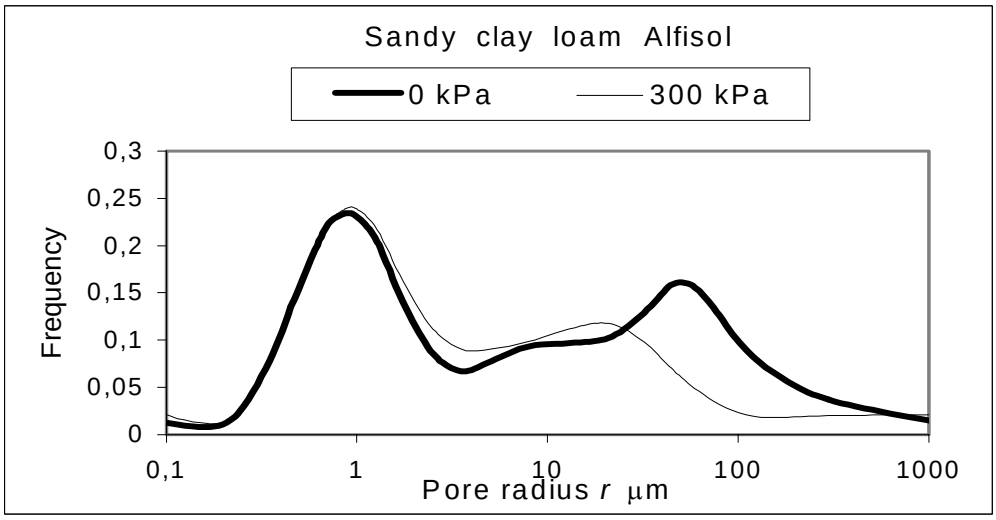

3.3.4. Pore size distribution: Application of equation (2)

Parameters of the soil water retention equation (2) obtained by optimization for all soils and all values of compression stresses are in Table 3. The fitted soil water retention curves with parameters of Table 3 resulted in a good agreement with the experimental data, see the Table 4 as one example.

Table 3
Parameters of Eq. (4) obtained by optimization for soils in Table 1.

Soil	Compr. stress,kPa	h_{m1}, cm Matrix	σ_1 Matrix	h_{m2}, cm Structural	σ_2 Structural
ENTISOL Loamy sand	0	887	1.73	58	0.86
	100	879	1.92	51	1.18
	200	811	1.81	59	0.91
	300	655	1.47	41	1.51
ENTISOL Sandy loam	0	2589	1.10	130	1.28
	100	3217	1.74	116	1.11
	200	2576	1.17	114	1.51
	300	2880	1.16	115	1.28
ALFISOL Sandy clay loam	0	3813	2.44	42	1.33
	100	3211	1.73	48	1.20
	200	6260	2.90	77	1.05
	300	4556	2.84	99	1.37
ALFISOL Sandy loam	0	2664	2.43	49	1.0
	100	2916	2.36	77	0.97
	200	2732	2.27	55	1.06
	300	2567	2.18	86	0.84
VERTISOL Clay loam	0	3058	2.05	29	1.33
	100	2978	1.44	18	1.09
	200	4256	2.69	37	1.41
	300	5462	2.41	46	1.40

Table 4
Measured soil water retention data and data obtained by optimization, Eqs. (4) and (6) with conditions (7) and (8) for sandy clay loam Alfisol.

Pressure head h cm	Compression 0 kPa		Compression 300 kPa	
	θ measured	θ computed	θ measured	θ computed
1	0,511	0,510	0,468	0,468
10	0,481	0,480	0,448	0,453
20	0,449	0,447	0,441	0,437
40	0,399	0,404	0,423	0,415
100	0,351	0,347	0,38	0,383
330	0,299	0,304	0,328	0,292
1000	0,249	0,218	0,271	0,255
3000	0,140	0,176	0,169	0,210
10000	0,109	0,127	0,140	0,159

Parameters in Table 3 document the change of the pore size distribution in individual domains for all studied soils and all values of compression stress.

The mean pressure head h_{m1} decreases with the increased compression in the matrix domain of loamy sand Entisol (Table 3), i.e. the peak of the equivalent pore radius r_{m1} is shifted to higher values of r with the compression (Table 5). The shift of r_{m1} is opposite in all remaining soils. The value of σ_1 does not change uniformly with the gradual increase of the compression. We find a following tendency: σ_1 is increasing in all soils except of clay loam Vertisol and loamy sand Entisol at 300 kPa compression.

In case of the structural domain the mean pressure head h_{m2} decreases with the increased compression in Entisols (Table 3), i.e. the position of the peak of the equivalent radius r_{m2} is shifted towards higher radii with the increase of the compression stress (Table 5). Alfisols and Vertisol behave differently. The shift of r_{m2} is either opposite or not changed (Table 5). The value of σ_2 does not change uniformly with the gradual increase of the compression in a similar way as it is in the matrix domain. The change has an increasing tendency due to the compression in Entisols and in Vertisol. The pore size distribution is more flat and more broadly extended due to the compression than in case of soils without compression. In the remaining soils there is an opposite tendency due to the compression, but the change is relatively small, see the example for sandy clay loam Alfisol. We assume that the different change of the pore size distribution after compression is due to the difference in aggregate stability mainly.

Table 5
Equivalent mean pore radius in matrix (r_{m1}) and structural (r_{m2}) domains. Equivalent pore radius at the separation of matrix and structural domains $r(h_A)$.

Soil	Compressive stress, kPa	r_{m1} μm	r_{m2} μm	$r(h_A)$ μm
ENTISOL Loamy sand	0	1.68	25.69	6.9
	100	1.70	29.21	7.6
	200	1.83	25.25	7.8
	300	2.27	36.34	10.9
ENTISOL Sandy loam	0	0.58	11.46	2.5
	100	0.46	12.84	2.7
	200	0.58	13.07	2.6
	300	0.52	12.96	2.6
ALFISOL Sandy clay loam	0	0.39	35.48	3.4
	100	0.46	31.04	4.0
	200	0.24	19.35	4.4
	300	0.33	30.41	4.0
ALFISOL Sandy loam	0	0.56	30.41	4.4
	100	0.51	19.35	3.7
	200	0.54	27.09	3.4
	300	0.58	17.32	4.0
VERTISOL Clay loam	0	0.49	51.37	4.1
	100	0.50	82.78	8.7
	200	0.35	40.27	4.0
	300	0.27	32.39	3.7

Parameters h_{mi} and σ_i were used for simulating pore size distributions in the structural and matrix domains of soils without compression and after compression. Since minor secondary peaks appear there and a distinct skewness exists in some of the experimental pore size distribution curves, the modeled pore size distribution curves do not copy the experimental ones. Data of two soils without compression and after compression 300 kPa are plotted in Figures 6 to 9 as examples of the modeled change induced by compression in the soil of poor structural development (loamy sand Entisol) and in the soil with a high aggregate stability (sandy clay loam Alfisol).

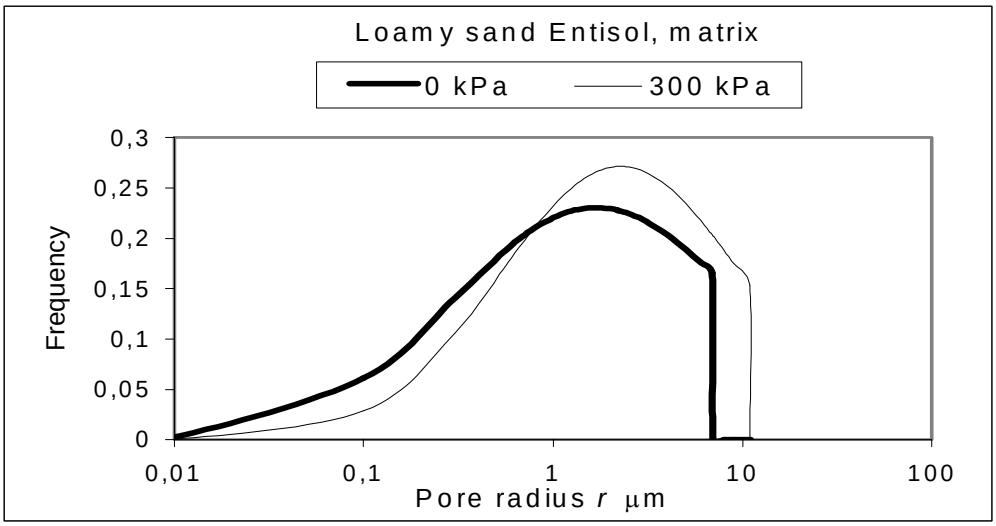

Fig. 6.

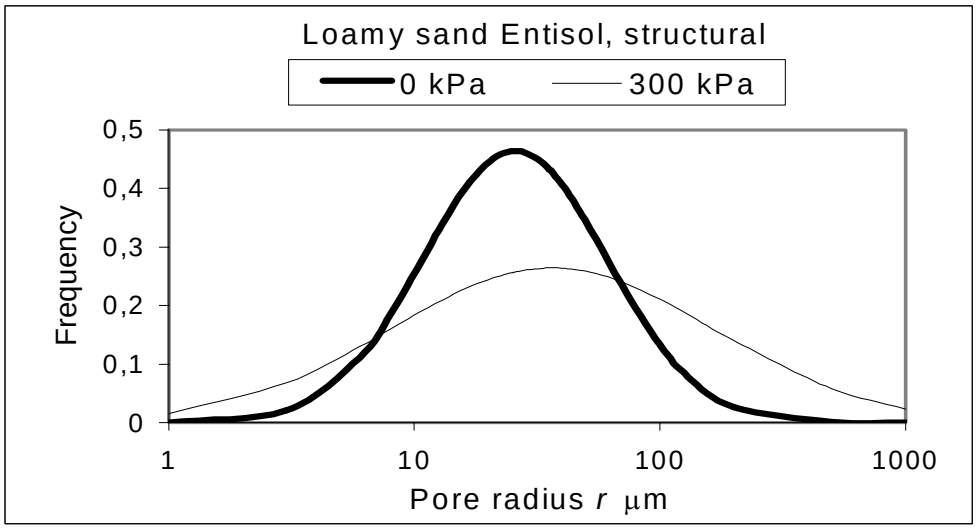

Fig. 7.

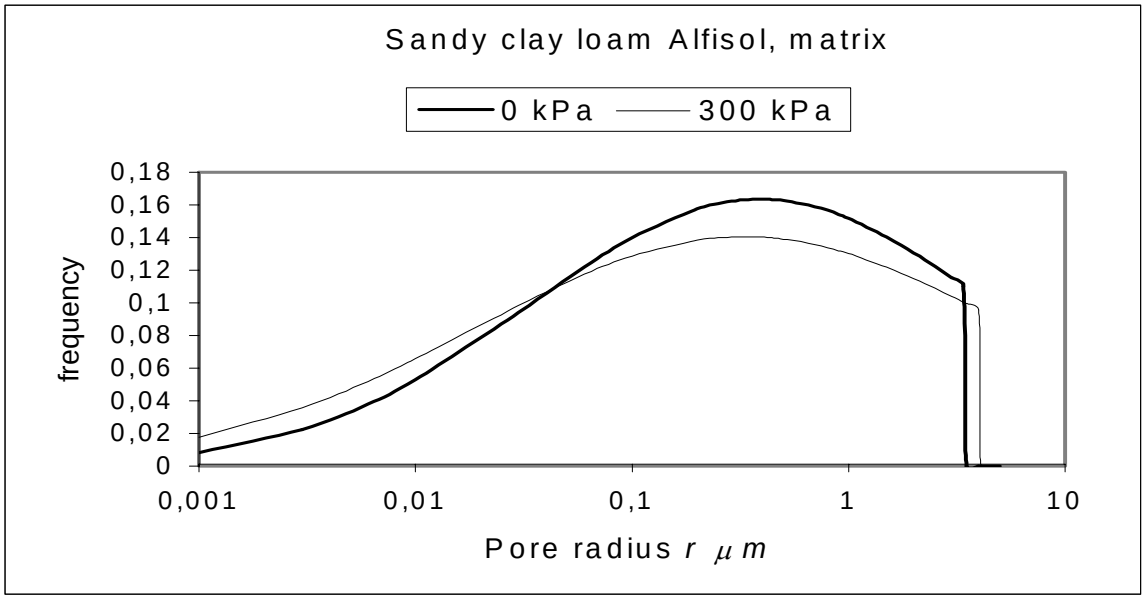

Fig. 8.

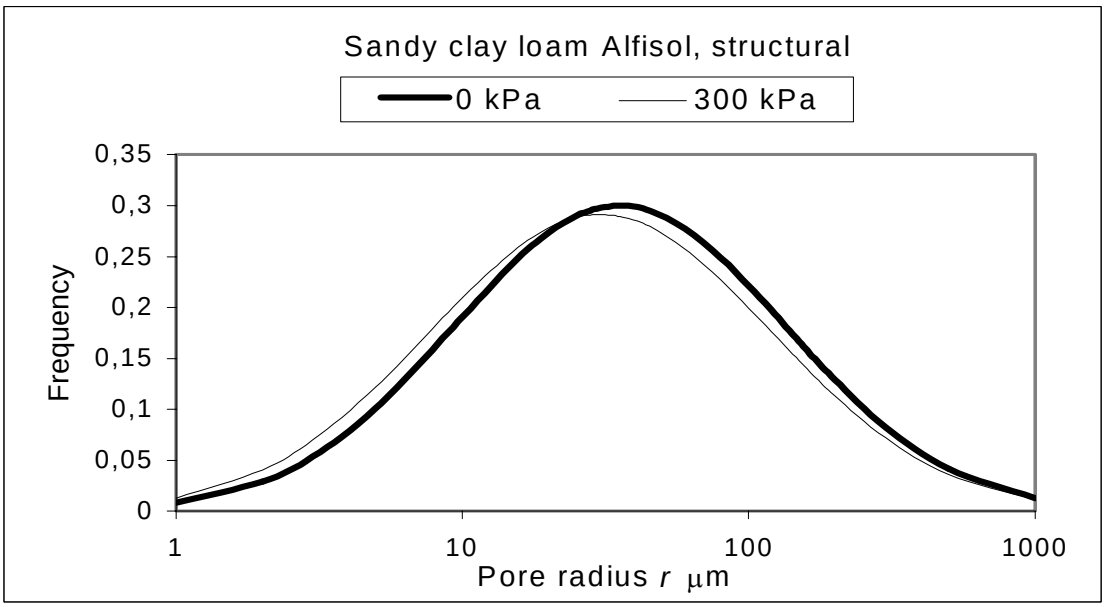

Fig. 9.

Pore size distribution in the matrix domain of Entisol (Fig. 6) is more influenced by the compression when compared to the change in Alfisol (Fig. 8) judging according to the modeled relationships. Pore size distribution in the structural domain of Entisol (Fig. 7) is very influenced by the compression, compared to slight change of the curve in Alfisol (Fig. 9). Let us note here that the experimental pore size distribution in Fig. 5 indicates a substantial change of the pore size distribution in the structural domain of Alfisol due to compression. It means that the model on log-normal distribution is not universal and it could be imperfect in

some instances. It is evident that the future research should test other types of probability density functions, too. We expect that close links to the study on soil micromorphology will contribute to the improvement of our recent models.

3.4. CONCLUSIONS

1. Soil water retention curves are significantly changed due to compression in soils of low aggregate stability. The change is substantially smaller in soils of high aggregate stability.
2. The value of pressure head h_A separating the structural pores from the matrix pores is in very broad ranges for various soil taxons and the applied compression. The boundary between soil pore categories can not be taken as a fixed value for all soils and all types of soil use.
3. The parameters of the pore size distribution in structural and matrix domains do not react in the same direction of increase or decrease due to the compression when individual soils are compared. The pore size distribution is changed substantially in structural as well in matrix domains of soils characterized by low aggregate stability. The change in the matrix domain is relatively small in soils with well developed structure and high aggregate stability, while the change is more expressed in the structural domain.

References

Ahuja, L.R., Nancy, J.W., Green, R.E., Nielsen, D.R., 1984. Macroporosity to characterize variabilty of hydraulic conductivity and effects of land management. Soil Sci. Soc. Am. J. 48, 670-699.

Assouline, S., Tessier, D., Tavares-Filho, J., 1997. Effect of compaction on soil physical and hydraulic properties: Experimental results and modeling. Soil Sci. Soc. Am,. J. 61, 390-398.

Brewer, R., 1964. Fabric and Mineral Analysis of Soils. John Wiley and Sons, New York.

Brutsaert, W., 1966. Probability laws for pore size distribution. Soil Sci. 101, 85-92.

Canarache, A., Trandafirescu, A., Colibas, J., 1984. Effect of induced compaction by wheel trafic on soil physical properties and yield of maize in Romania. Soil Tillage Res. 4, 199-213.

Clothier, B.E. and White, I., 1981. Measurement of sorptivity and soil water diffusivity in the field. Soil Sci. Soc. Am. J. 45, 241-285.

Durner, W., 1992. Predicting the unsaturated hydraulic conductivity using multi-porosity water retention curves. In: van Genuchten, M.Th., Leij, F.J. and Lund, L.J. (Eds.), Indirect Methods for Estimating the Hydraulic Properties of Unsaturated Soils. University of California, Riverside, CA, USA, pp.185-202.

Flint, L.E., Flint, A.L., 2002. Pore size distribution. In: Dane, J.H., Topp, G.C. (Co-Eds), Methods of Soil Analysis. Part 4. Physical Methods. Soil Science Society of America, Madison, Wisconsin, USA, pp.246-253.

Greenland, D.J., 1981. Soil management and soil degradation. J. Soil Sci. 32, 301-322.

Horn, R., 1994. The effect of aggregation of soils on water, gas and heat transport. In: Schulze, E.D. (Ed.), Flux Control in Biological Systems, Academic Press, 10, pp. 335-361.

Horn,R., Baumgartl, T., Kayser, R. and Baasch, S., 1995. Effect of Aggregate strength on changes in strength and stress distribution in structured bulk soils. In: Hartge, K.H. and Stewart, R. (Eds.), Soil Structure – its Development and Function. Advances in Soil Science, pp. 31 – 52.

Kosugi, K., 1994. Three-parameter lognormal distribution model for soil water retention. Water Resour. Res. 30, 891-901.

Kosugi, K. and Inoue, M., 1999. Analysis of soil water movement by using a generalized model for unsaturated hydraulic conductivity (in Japanese). Proc. 11 Ann. Conf. Joint Research Program, The Arid Land Research, Tottori Un., pp. 71-72 , quoted according to personal communication.

Kutílek, M., 2004. Soil hydraulic properties as related to soil structure. Soil Tillage Res. 79, 175-184.

Kutílek, M. and Nielsen, D.R., 1964. Soil Hydrology. Catena Verlag, Cremlingen Destedt, Germany.

Kutílek, M, Jendele, L. and Panayiotopoulos, K.P., 2006. The influence of uniaxial compression upon pore size distribution in bi-modal soils. Soil Till. Res. 86,27-37.

Leij, F.J., Ghezzehei, T.A., Or, D., 2002. Modeling the dynamics of the soil pore-size distribution. Soil Tillage Res. 64, 61-78.

Luxmoore, R.J., 1981. Micro-, meso- and macroporosity of soil. Soil Sci. Soc. Am. J. 45, 241-285.

Mapa, R.B., Green, R.E., Santo, L., 1986. Temporal variability of soil hydraulic properties with wetting and drying subsequent to tillage. Soil Sci. Soc. Am. J. 50, 1133-1138.

Othmer, H., Diekkrüger, B. and Kutílek, M., 1991. Bimodal porosity and unsaturated hydraulic conductivity. Soil Sci. 152, 139-150.

Pachepsky, Ya.A., Mironenko, E.V. and Schcherbakov, R.A., 1992. Prediction and use of soil hydraulic properties. In: van Genuchten, M.Th., Leij, F.J. and Lund, L.J. (Eds.), Indirect Methods for Estimating the Hydraulic Properties of Unsaturated Soils. Univ. of California, Riverside, CA, U.S.A., pp. 203-213.

Pagliai, M., Pellegrini, S., Vignozzi, N., Rousseva, S., Graselli, O., 2000. The quantification of the effect of subsoil compaction on soil porosity and related physical properties under conventional and reduced management practices. Advances in GeoEcology 32, 305-313.

Pagliai, M. and Vignozzi, N., 2002. Image analysis and microscopic techniques to characterize soil pore system. In: Blahovec, J. and Kutílek, M. (Eds.), Physical Methods in Agriculture, Kluwer Academic Publishers, London, pp. 13-38.

Panayiotopoulos, K.P., Salonikiou, E., Siaga, K., Germanopoulou, V., and Skaperda, S., 2003. Effect of uniaxial compression on water retention, hydraulic conductivity and the penetration resistance of six Greek soils. Int. Agrophysics 17, 191-197.

Panayiotopoulos, K.P., Kostopoulou, S., and Hatjiyiannakis, E., 2004. Variation of physical and mechanical properties with depth in Alfisols. Int. Agrophysics 18, 55-63.

Powell, M.J.D., 1977. Restart procedures for the conjugate gradient method. Mathematical Programming 12, 241-254.

Powell, M.J.D., 1978. A fast algorithm for nonlinearly constrained optimization calculations. In: Watson, G.A. (Ed.) Lecture Notes in Mathematics, p, 630, Springer-Verlag,
Berlin, Germany, 144-157.

Tuller, M. and Or, D., 2002. Unsaturated hydraulic conductivity of structured porous media. A review. Vadose Zone J. 1, 14-37.

Zeiliguer, A.M., 1992. Hierarchical system to model the pore structure of soils: Indirect methods for evaluating the hydraulic properties. In: van Genuchten, M.Th., Leij, F.J. and Lund, L.J. (Eds.) Indirect Methods for Estimating the Hydraulic Properties of Unsaturated Soils. University of California, Riverside, CA.